

## Optical waveguiding in BaTiO<sub>3</sub>/MgO/Al<sub>x</sub>O<sub>y</sub>/GaAs heterostructures

D. Chen, T. E. Murphy, S. Chakrabarti, and J. D. Phillips<sup>a)</sup>

Department of Electrical Engineering and Computer Science, University of Michigan, Ann Arbor, Michigan 48109-2122

(Received 8 June 2004; accepted 11 October 2004)

Thin films of BaTiO<sub>3</sub> with MgO buffer layers were deposited on patterned GaAs substrates incorporating Al<sub>x</sub>O<sub>y</sub> for optical confinement. The inclusion of Al<sub>x</sub>O<sub>y</sub> layers are used to provide a means for obtaining thick optical confinement layers as a substitute for MgO cladding layers which have large thermal expansion mismatch with respect to GaAs and BaTiO<sub>3</sub> that typically result in thin film cracking. Deposition on patterned features was found to reduce thin film cracking and is attributed to a reduction in thin film stress resulting from thermal expansion mismatch. A maximum ridge width of 10–20 μm is estimated for 1-μm-thick BaTiO<sub>3</sub> thin films. Optical waveguiding was observed in BaTiO<sub>3</sub>/MgO/GaAs/Al<sub>x</sub>O<sub>y</sub>/GaAs ridges suggesting the potential application of these structures for integrated optoelectronics. © 2004 American Institute of Physics.  
[DOI: 10.1063/1.1828212]

The integration of ferroelectric oxide materials on GaAs would provide capabilities for multifunctional devices and integrated optoelectronics. Ferroelectric oxides such as BaTiO<sub>3</sub> are transparent in the visible and infrared and possess strong electro-optic coefficients making them attractive for active and passive optical components. The development of optical waveguide devices based on ferroelectric/GaAs integration faces several challenges including chemical and mechanical incompatibilities and the achievement of the proper refractive index contrast to prevent leakage of the optical wave to the substrate. The use of MgO buffer layers has been shown to mitigate some of these challenges. Magnesium oxide provides an excellent barrier to diffusion, may be grown epitaxially at low temperatures (~350 °C), and possesses a near 4:3 commensurate lattice match to GaAs and is a compatible substrate for BaTiO<sub>3</sub> deposition.<sup>1–4</sup> Recently, electro-optic devices have been demonstrated in BaTiO<sub>3</sub> thin films deposited on MgO substrates.<sup>5,6</sup> The realization of BaTiO<sub>3</sub>/MgO/GaAs heterostructures still faces two primary challenges prior to the realization of integrated optical devices: the reduction or elimination of thin film cracking due to thermal expansion mismatch,<sup>7</sup> and the incorporation of optically thick buffer layers with low refractive index for waveguiding. In this work, the incorporation of Al<sub>x</sub>O<sub>y</sub> buffer layers and the deposition of BaTiO<sub>3</sub>/MgO thin films on prepatterned GaAs substrates are presented to address these challenges. The demonstration of optical waveguiding in BaTiO<sub>3</sub>/MgO/GaAs/Al<sub>x</sub>O<sub>y</sub>/GaAs mesa structures is presented.

The structural design for optical waveguiding in BaTiO<sub>3</sub> thin films on GaAs is shown schematically in Fig. 1. This design features the incorporation of Al<sub>x</sub>O<sub>y</sub> buffer layers obtained through the wet oxidation of AlGaAs.<sup>8</sup> This technique provides a means of achieving a thick buffer layer with low refractive index ( $n \sim 1.7$ ), while maintaining a thin GaAs layer for the growth of MgO buffer layers and the BaTiO<sub>3</sub> thin film of interest. The layer structure provides a means for optical confinement in the vertical direction. Optical confinement in the lateral direction is achieved in this design

through photolithographic patterning. The fabrication procedure for achieving the designed ridge waveguide structures is outlined in the following. First, GaAs/Al<sub>0.98</sub>Ga<sub>0.02</sub>As/GaAs layers (30 nm/500 nm/200 nm) were grown by molecular beam epitaxy on GaAs (001) substrates. Ridge waveguide patterns of width ranging from 3 to 60 μm were defined by standard photolithography and transferred using reactive ion etching using a BCl<sub>3</sub>/Ar etch chemistry. Samples were etched to depths ranging from 80 nm (just through the GaAs cap) to 1 μm (completely through the AlGaAs). A wet oxidation step was then performed at a temperature of 420 °C for 1 h to oxidize the AlGaAs material under the ridges. After oxidation, MgO and BaTiO<sub>3</sub> thin films were deposited by pulsed laser deposition using an excimer laser ( $\lambda = 248$  nm, 25 ns pulse width, 10 Hz,  $\sim 2$  J/cm<sup>2</sup>). The MgO buffer layers were deposited at a substrate temperature of 450 °C and oxygen partial pressure of  $1.5 \times 10^{-4}$  using a Mg target. The BaTiO<sub>3</sub> thin films were deposited at a substrate temperature of 600 °C and oxygen partial pressure of 10 mT using a BaTiO<sub>3</sub> target. The estimated thickness of MgO and BaTiO<sub>3</sub> were determined to be 20 and 1000 nm, respectively. X-ray diffraction scans ( $\theta$ - $2\theta$ ) were used to determine the crystalline characteristics of the thin films. A majority of the surface area of the patterned samples contains regions outside of the ridges, where x-ray diffraction scans will probe material deposited on the etched and oxidized amorphous Al<sub>x</sub>O<sub>y</sub> surface. The thin film materials deposited on the GaAs surface on top of the ridges are of higher quality, but cannot be probed directly by x-ray diffraction in the absence of ad-

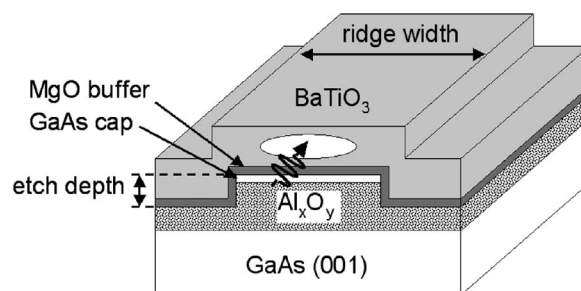


FIG. 1. Schematic of BaTiO<sub>3</sub> ridge waveguide structure.

<sup>a)</sup>Electronic mail: jphilli@engin.umich.edu

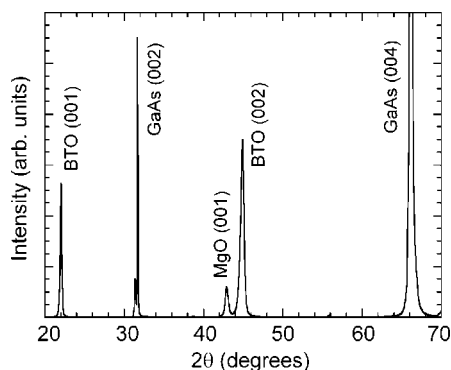
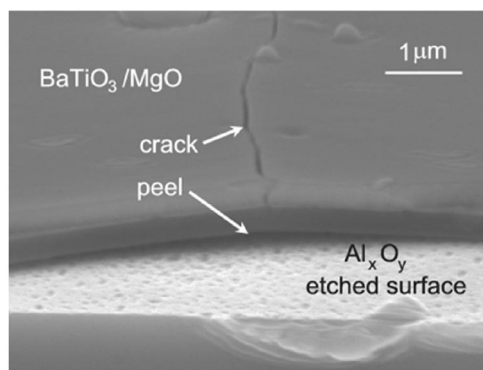


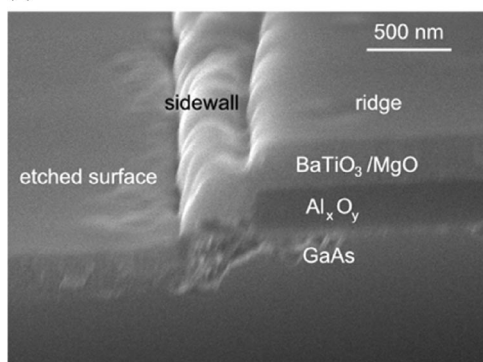
FIG. 2. X-ray diffraction scan of BaTiO<sub>3</sub>/MgO thin film on GaAs (001) demonstrating crystalline material with preferred orientation.

vanced focusing optics. BaTiO<sub>3</sub>/MgO thin film deposition on GaAs substrates was used as an indicator of material quality deposited on top of ridges, where an x-ray diffraction scan of BaTiO<sub>3</sub>/MgO thin film structure deposited on GaAs under similar conditions is shown in Fig. 2.

The design and fabrication procedure described intrinsically provides a means of reducing problems associated with the large mismatch in thermal expansion coefficients between GaAs ( $\alpha=5.73 \times 10^{-6}/\text{K}$  at 300 K), MgO ( $\alpha=11.15 \times 10^{-6}/\text{K}$  at 300 K), and BaTiO<sub>3</sub> ( $\alpha=6.5 \times 10^{-6}/\text{K}$  at 300 K).<sup>7</sup> The largest thermal expansion mismatch is between MgO and the other materials, suggesting that the thickness of the MgO buffer layer should be minimized. In addition, the difference in deposition temperature between MgO and BaTiO<sub>3</sub> should be minimized. A separate set of experiments was used to determine the effect of MgO thickness on sub-

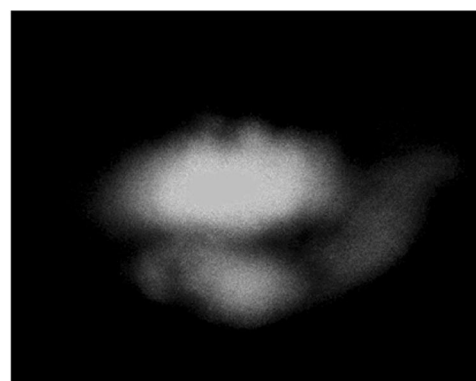


(a)

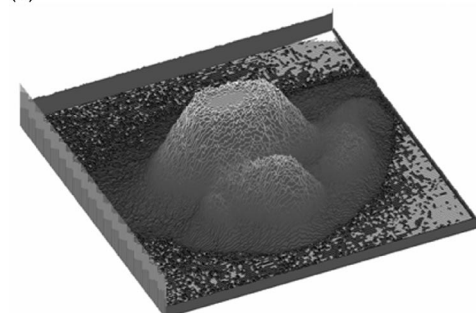


(b)

FIG. 3. Scanning electron microscope images of BaTiO<sub>3</sub>/MgO/GaAs/Al<sub>x</sub>O<sub>y</sub>/GaAs structures exhibiting (a) cracking in arbitrary directions on wide stripes and (b) predominant cracking perpendicular to patterning on a narrow stripe.



(a)



(b)

FIG. 4. Output from 10- $\mu\text{m}$ -wide BaTiO<sub>3</sub> ridge waveguides (a) captured by a digital camera and (b) intensity plot constructed from the digital image.

sequent BaTiO<sub>3</sub> thin film deposition. MgO/GaAs thin films of varying thickness were annealed at 600 °C for 2 h after deposition to simulate the thermal treatment during BaTiO<sub>3</sub> deposition. MgO buffer layers with thickness of approximately 20 nm were found to be suitable for subsequent BaTiO<sub>3</sub> deposition at 600 °C, where MgO thin films of approximately 80 nm exhibited peeling and cracking. A target thickness of 20 nm for MgO buffer layers was used for subsequent experiments.

The BaTiO<sub>3</sub>/MgO thin films deposited on the patterned GaAs/Al<sub>x</sub>O<sub>y</sub>/GaAs structures were found to exhibit cracking and peeling dependent upon ridge width. An illustration of cracking and peeling in these materials is shown in Fig. 3(a). Significant cracking is observed on wide ridges. Cracking is observed in all directions in-plane for the wide ridges, but is greatly reduced and confined to the direction perpendicular to the patterned ridge for small ridge width. The crack spacing for the small ridge width is  $>7 \mu\text{m}$ , suggesting that the cracks negligibly interact.<sup>9</sup> A cross-sectional scanning electron microscope image of the thin film structure on the patterned substrates is shown in Fig. 3(b). The reduced cracking for narrower ridges is attributed to strain relief in the direction perpendicular to the patterned ridge, where the strain profile becomes more uniaxial. This behavior is supported by the model presented by Suhir,<sup>10</sup> where cracking will result beyond a critical stress and the thermal stress increases with ridge width. Experimentally, the maximum ridge width prior to cracking was found to be between 10 and 20  $\mu\text{m}$  for a 1- $\mu\text{m}$ -thick BaTiO<sub>3</sub> layer. The cracking does not appear to have a strong dependence on etch depth for the dimensions studied, though a few scattered ridges exhibited peeling that appeared to be more prevalent for wide ridges with deeper etches. This behavior is not understood at this time.

A selected sample with 1- $\mu\text{m}$ -thick  $\text{BaTiO}_3$ , 20-nm-thick  $\text{MgO}$ , and an etch depth of 100 nm was studied for optical waveguiding. This sample was thinned mechanically to 200  $\mu\text{m}$ , scribed, and cleaved to provide facets for optical coupling. Visible light was coupled into the  $\text{BaTiO}_3$  ridges by end-firing with a frequency doubled Nd:YAG laser ( $\lambda = 532$  nm). An elliptical output beam was observed when coupling light into the waveguides, where the output captured by a digital camera for a 10- $\mu\text{m}$ -wide ridge of length 1 mm is shown in Fig. 4(a). The output beam is multimode, where numerous guided modes are estimated using the effective index approximation. An intensity plot constructed from the digital image is shown in Fig. 4(b). The output light shows additional optical guiding adjacent to the elliptical output beam. The additional light output may be attributed to guiding in the  $\text{Al}_x\text{O}_y$  layer or  $\text{BaTiO}_3$  material on the sidewalls of the ridges. A measurement of optical power traveling through coupling and collection optics with and without the waveguide present resulted in values of 110 and 6 mW. The observed efficiency of 5.45% represents coupling loss, reflection and losses at facets, and waveguide losses. Light scattering in the waveguide material was observed at defects present in the  $\text{BaTiO}_3$  material produced by the pulsed laser deposition process.

In conclusion, ridge waveguides consisting of  $\text{BaTiO}_3/\text{MgO}/\text{GaAs}/\text{Al}_x\text{O}_y/\text{GaAs}$  layer structures were investigated. The use of  $\text{Al}_x\text{O}_y$  layers and thin film deposition

on patterned substrates provide a means of obtaining  $\text{BaTiO}_3$  thin films and optical confinement layers of suitable thickness for optical waveguiding on GaAs substrates. Optical waveguiding was observed in these structures showing primary optical confinement in the  $\text{BaTiO}_3$  thin film. Further study of optical losses and electro-optic properties of these structures are desired to determine their suitability for integrated optoelectronics.

This work is supported by the National Science Foundation under Grant No. ECS-0238108.

- <sup>1</sup>K. Nashimoto, D. Fork, and T. H. Geballe, *Appl. Phys. Lett.* **60**, 1199 (1992).
- <sup>2</sup>E. J. Tarsa, X. H. Wu, J. P. Ibbetson, J. S. Speck, and J. J. Zinck, *Appl. Phys. Lett.* **66**, 3588 (1995).
- <sup>3</sup>S. W. Robey, *J. Vac. Sci. Technol. A* **16**, 2423 (1998).
- <sup>4</sup>M. Hong, M. Passlack, J. P. Mannaerts, J. Kwo, S. N. G. Chu, N. Moriya, S. Y. Hou, and V. J. Fratello, *J. Vac. Sci. Technol. B* **14**, 2297 (1996).
- <sup>5</sup>D. M. Gill, C. W. Conrad, G. Ford, B. W. Wessels, and S. T. Ho, *Appl. Phys. Lett.* **71**, 1783 (1997).
- <sup>6</sup>A. Petraru, J. Schubert, M. Schmid, and C. Buchal, *Appl. Phys. Lett.* **81**, 1375 (2002).
- <sup>7</sup>V. Srikant, E. J. Tarsa, D. R. Clarke, and J. S. Speck, *J. Appl. Phys.* **77**, 1517 (1995).
- <sup>8</sup>K. D. Choquette, K. M. Geib, C. I. H. Ashby, R. D. Twisten, O. Blum, H. Q. Hou, D. M. Follstaedt, B. E. Hammons, D. Mathes and R. Hull, *IEEE J. Sel. Top. Quantum Electron.* **3**, 916 (1997).
- <sup>9</sup>M. D. Thouless, *Annu. Rev. Mater. Sci.* **25**, 69 (1995).
- <sup>10</sup>E. Suhir, *Int. J. Solids Struct.* **27**, 1025 (1991).